

# SIS100 Project Note, WP 2.8.1 SIS100 Beam Dynamics

## Overview of the Longitudinal Beam Dynamics for the SIS100 Proton Cycles

V. Kornilov, O. Boine-Frankenheim, D. Ondreka,  
FAIR@GSI, GSI Helmholtzzentrum, Darmstadt, Germany

July 25, 2013

### 1 Summary

Two alternative SIS100 proton scenarios are discussed presently, with  $\gamma_t = 18.3$  in the ramp beginning and with  $\gamma_t = 45.5$  afterward, and with the transition crossing at  $\gamma_t = 8.9$ . The initial longitudinal bunch area  $A_z = \pi\epsilon_z$  is given by the injection of the four bunches from SIS18, each provided by the full SIS18 circumference with the momentum spread  $\delta_{\max} = \pm 0.001$  from the p-linac at the energy of  $E_K = 70$  MeV,

$$A_z = 4 \times p_0 C 2\delta_{\max} = 4 \times 0.53 \text{ eV-s} = 2.13 \text{ eV-s}, \quad (1)$$

the corresponding total emittance is  $\epsilon_z = 0.68$  eV-s. We try to find the largest possible emittance increase in order to mitigate the intensity effects. As a restriction we assume the momentum acceptance  $\delta_{\max} = \Delta p_{\max}/p = \pm 0.005$ , the reference rf voltage is  $V_0 = 300$  kV.

First we discuss the cycle with the shifted  $\gamma_t$  which has no transition. One bunch is accelerated with  $h = 5$  from the initial full bunch length  $t_b = 250$  ns and reaches the design length  $t_b = 50$  ns at the extraction energy, see Fig. 5 and the corresponding discussion. The momentum spread exceeds the acceptance at the ramp beginning, but a proper rf ramp may help. A more challenging problem can be due to the microwave instability. The Boussard criterion Eq. (7) predicts that the stability boundary decreases below  $10 \Omega$  due to the very small  $\eta$  close to the end of the ramp, see Fig. 6. At the CERN PS, which can be taken as a similar synchrotron, the inductive broad-band impedance  $Z_{\parallel}/n \approx i20 \Omega$  has been repeatedly measured [2]. The space-charge impedance  $Z_{\parallel}/n = iZ_0 g_0 / (2\beta\gamma^2)$  is inductive below the transition but it decreases rapidly along the ramp, see Fig. 6, left. Once outside the Landau damped region, the bunch can be strongly unstable, see Fig. 6, right.

For the proton cycle with the transition crossing we consider two scenarios of the longitudinal emittance and we always compare the  $h = 5$  one-bunch acceleration with the  $h = 10$  four-bunch acceleration. The longitudinal emittance conservation, which we use for the calculations in the present report, is not valid for the nonadiabatic region near transition. The beam dynamics near transition is beyond the scope of this report, thus we indicate where appropriate the nonadiabatic region, given by the nonadiabatic time. This can be calculated by [1]

$$T_c = \left( \frac{\beta_t^2 \gamma_t^4 |\tan \phi_s|}{2\omega_0 h \dot{\gamma}^2} \right)^{1/3}. \quad (2)$$

For the SIS100 ramp it provides  $T_c = 3.6$  ms for  $h = 10$  and  $T_c = 4.53$  ms for  $h = 5$ . Thus we indicate the nonadiabatic region in the plots of the bunch parameters near transition.

The effect of the chromatic nonlinearity is due to the large momentum particles reaching the transition  $\eta = \eta_0 + \eta_1 \delta_{\max} = 0$  while the synchronous particle is still below the transition. This time difference is called the nonlinear time and can be calculated by

$$T_{nl} = \frac{\gamma_t \alpha_1 \delta_{\max}}{2\dot{\gamma}}, \quad (3)$$

where  $\alpha_1 = \eta_1 \gamma_t^2$ . Assuming  $\alpha_1 = 2$  it provides  $T_{nl} = 0.4$  ms for  $h = 10$  and  $T_{nl} = 0.7$  ms for  $h = 5$ . Since the nonlinear time is smaller than the nonadiabaticity time the related emittance growth can be estimated as [3]

$$\frac{\Delta\epsilon_z}{\epsilon_z} \approx 0.76 \frac{T_{nl}}{T_c}, \quad (4)$$

which is equal to 0.09 for  $h = 10$  and 0.12 for  $h = 5$ .

The effect of the space-charge mismatch at the transition is due to the different sign of the longitudinal space-charge force below and above the transition. The corresponding space-charge parameter is the ratio of the space-charge force to the rf force and can be calculated by [1]

$$\eta_{sc} = \frac{9\Gamma^3(\frac{1}{3}) N_p r_0 g_0}{16\sqrt{2} R} \left( \frac{\beta_t E_{\text{rest}}}{A_z \omega_0} \right)^{3/2} \left( \frac{\omega_0}{\beta_t \dot{\gamma}} \right)^{1/2}. \quad (5)$$

The space-charge parameter  $\eta_{sc} = 2$  is quite strong, it causes the bunch length oscillations with the amplitude above the double of the initial bunch length [1].

The first scenario with transition assumes a matched bunch at the extraction, with a longitudinal emittance increase to  $\epsilon_z = 0.85$  eV-s ( $A_z = 2.67$  eV-s), see Figs. 7–9. The bunches are very short near transition,  $t_b = 41$  ns for the  $h = 5$  one-bunch acceleration and

$t_b = 17$  ns for the  $h = 10$  four-bunch acceleration. The bunches can then be unstable not only near transition, but also during the rest of the ramp after transition, see Fig. 9. The mismatch space-charge parameters are very large,  $\eta_{sc} = 3.3$  for one-bunch and  $\eta_{sc} = 6.7$  for four-bunch.

The second scenario with transition supposes a larger longitudinal emittance increase, up to  $\epsilon_z = 2.22$  eV-s ( $A_z = 6.97$  eV-s), with a necessary bunch compression before extraction. The momentum spread for the  $h = 5$  one-bunch acceleration exceeds the momentum acceptance before and shortly after the transition, see Fig. 11. If this problem can be handled by the choice of the rf ramp, the  $h = 5$  one-bunch acceleration might be preferential because the  $h = 10$  four bunches can be unstable near and after the transition until the end of the ramp, see Fig. 12. Also, the mismatch space-charge parameter is moderate for the one-bunch acceleration,  $\eta_{sc} = 0.8$  and can be easier treated by the longitudinal feedback.

## 2 The Ramp in the SIS100 Proton Cycles

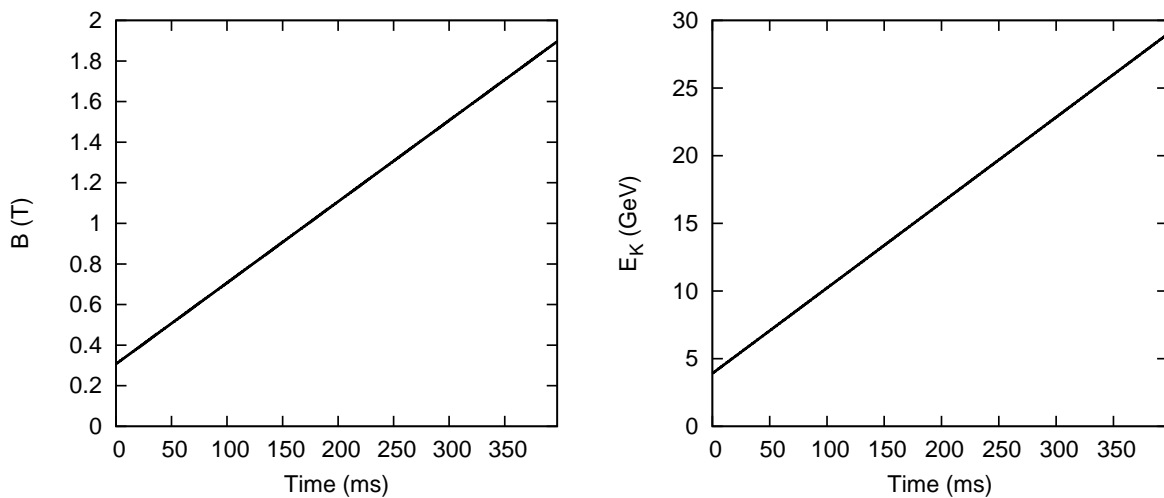


Figure 1: The bending magnetic field (left-hand side) and the proton kinetic energy (right-hand side) during the acceleration.

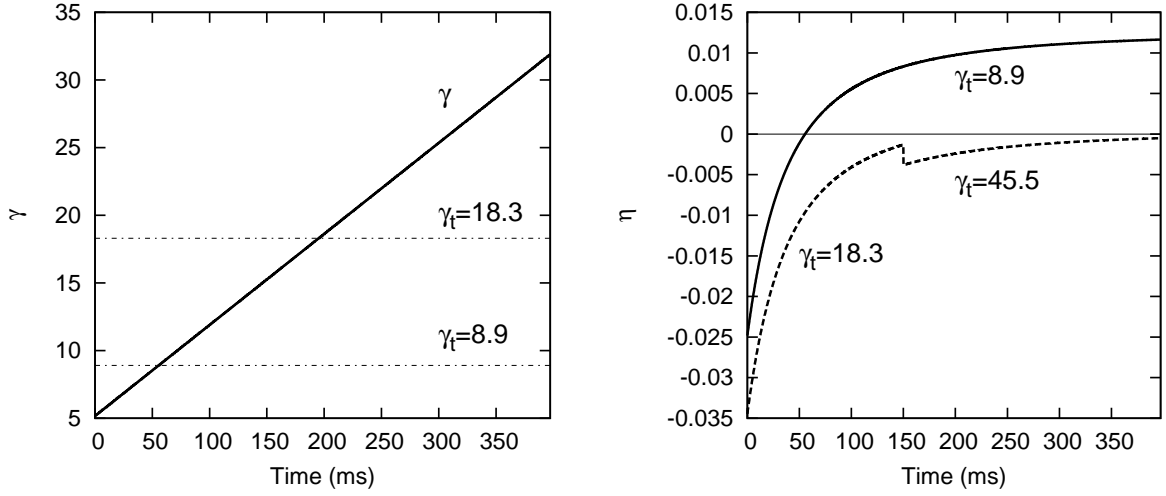


Figure 2: The relativistic Lorentz factor (left-hand side plot) and the slip factor  $\eta = 1/\gamma_t^2 - 1/\gamma^2$  (right-hand side plot) during the acceleration. The right-hand side plot: the full line is for  $\gamma_t = 8.9$ , the dashed line shows the case with  $\gamma_t = 18.3$  until Ramp Time 150 ms and with  $\gamma_t = 45.5$  afterward.

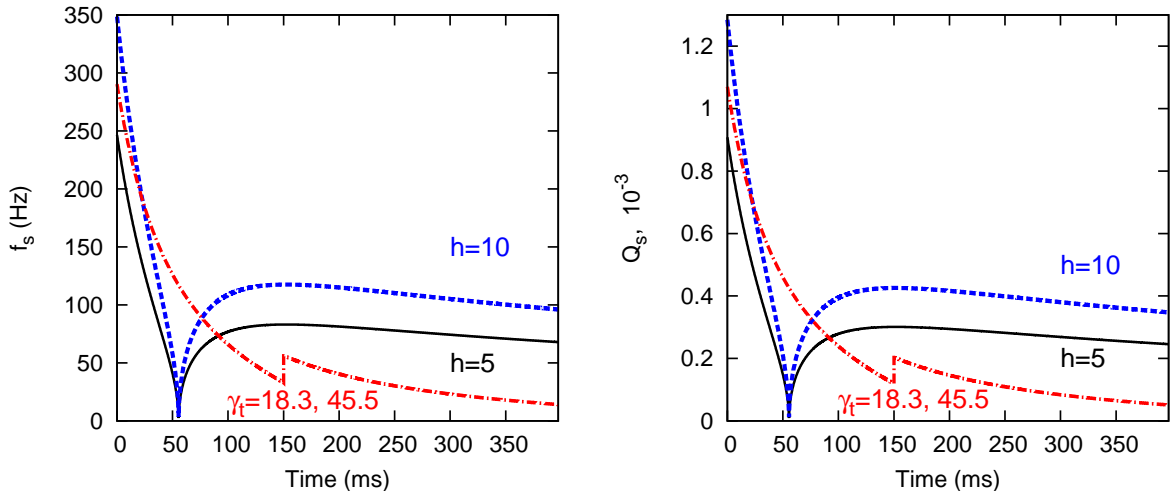


Figure 3: The synchrotron frequency (left-hand side plot) and the synchrotron tune (right-hand side plot) during the acceleration,  $V_0 = 300$  kV. The black ( $h = 5$ ) and the blue ( $h = 10$ ) lines are for  $\gamma_t = 8.9$ . The red line is for  $\gamma_t = 18.3$  until Ramp Time 150 ms and for  $\gamma_t = 45.5$  afterward, both with  $h = 5$ .

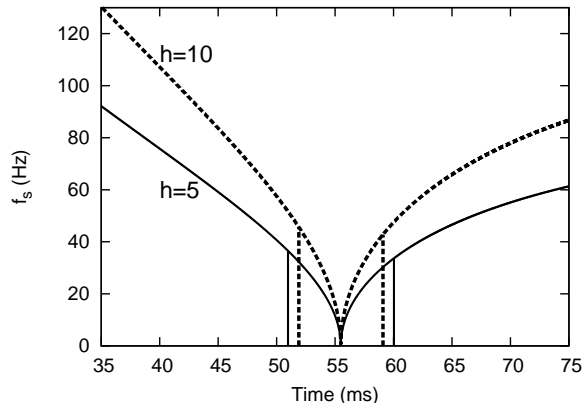


Figure 4: The synchrotron frequency near transition for  $h = 5$  (the solid line) and for  $h = 10$  (the dashed line) from Fig. 3, left. The vertical lines indicate the corresponding nonadiabaticity regions.

### 3 Proton Cycle with the Shifted $\gamma_t = 45.5$

The largest bunch area is given by the momentum acceptance  $\delta_{\max} = \pm 0.005$  and by the full bunch length  $t_b = 50$  ns at the extraction energy  $E_K = 29$  GeV,

$$A_z = \pi p_0 \frac{t_b \beta c}{2} \delta_{\max} = 11.75 \text{ eV-s}, \quad (6)$$

the corresponding emittance is  $\epsilon_z = 3.74$  eV-s. This means an increase by a factor of 5.5 with regards to the initial bunch area  $A_z = 2.13$  eV-s. A matched bunch with this parameters for  $\phi_s = 0$  can be achieved by a smaller rf voltage,  $V_0 = 249$  kV instead of  $V_0 = 300$  kV. For the rest of the ramp we always assume  $V_0 = 300$  kV,  $h = 5$ . In the beginning of the ramp the momentum deviation is larger than 0.005, see Fig. 5. This should still be manageable because the cycle with the shifted  $\gamma_t$  has a larger acceptance than the transition cycle, and it can be improved by the proper rf ramp. the acceptance  $\delta_{\max} = \pm 0.005$ , see Fig. 5,

Figure 6, left, shows the maximum longitudinal impedance for the stability of the microwave instability as given by the Boussard criterion [1],

$$\left| \frac{Z_{\parallel}}{n} \right|_{\max} = \frac{2\pi |\eta| \gamma m \beta^2 c^2}{q I_{\text{peak}}} \delta_{\text{rms}}^2, \quad (7)$$

while Fig. 6, right, presents the growth time of this instability assuming  $f_r = 2.8$  GHz (the cutoff frequency) and  $Z_{\parallel}/n = i10 \Omega$ .

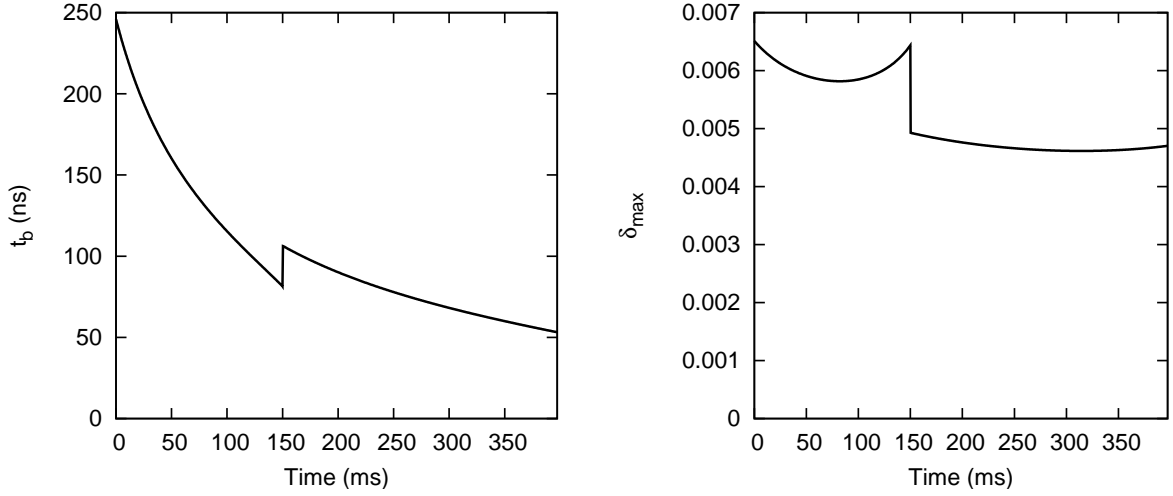


Figure 5: The full bunch length (left) and the half momentum spread (right) for the cycle with  $\gamma_t = 18.3$  until Ramp Time 150 ms and with  $\gamma_t = 45.5$  afterward. The longitudinal bunch area is  $A_z = 11.75$  eV-s.

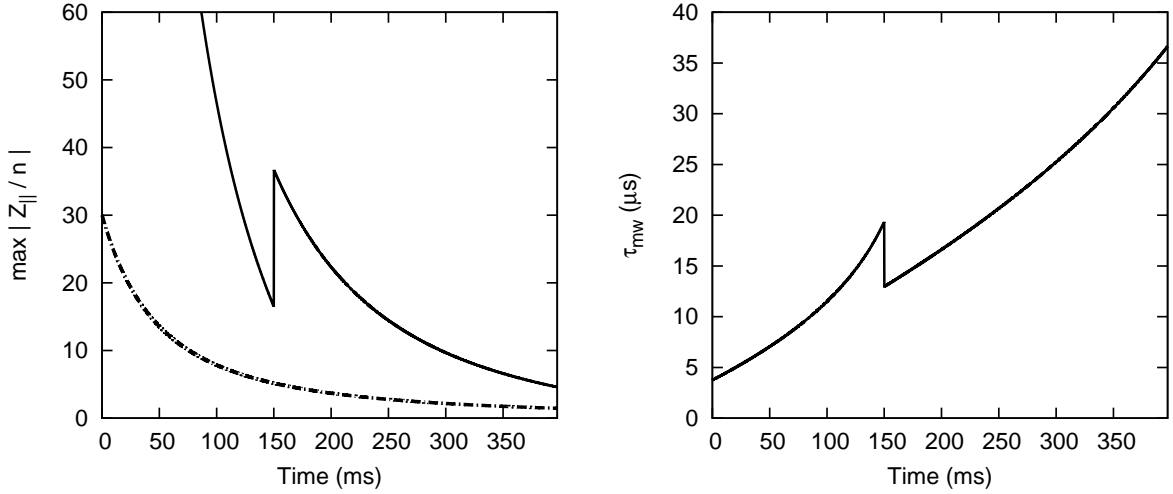


Figure 6: Left-hand side plot: stability boundary of the Boussard criterion (the full line) for the longitudinal microwave instability for the cycle with  $\gamma_t = 18.3$  until Ramp Time 150 ms and with  $\gamma_t = 45.5$  afterward; the chain line shows the longitudinal space-charge impedance. The longitudinal bunch area is  $A_z = 11.75$  eV-s. Right-hand side plot: the growth time of the microwave instability.

## 4 Matched Bunch at the Extraction for the Cycle with $\gamma_t = 8.9$

For a matched bunch at the extraction energy the final bunch length  $t_b = 50$  ns gives a constraint on the final momentum spread and on the corresponding maximum emittance  $\epsilon_z = 0.85$  eV-s ( $A_z = 2.67$  eV-s, an increase by a factor 1.25) which provides

one bunch	four bunches
$h = 5$	$h = 10$
$\epsilon_z = 0.85$ eV-s	$\epsilon_z = 0.21$ eV-s
$\eta_{sc} = 3.3$	$\eta_{sc} = 6.7$
$t_b = 50$ ns (at extr)	$t_b = 21$ ns (at extr)
$\delta_{max} = 1.1 \times 10^{-3}$ (at extr)	$\delta_{max} = 0.68 \times 10^{-3}$ (at extr)

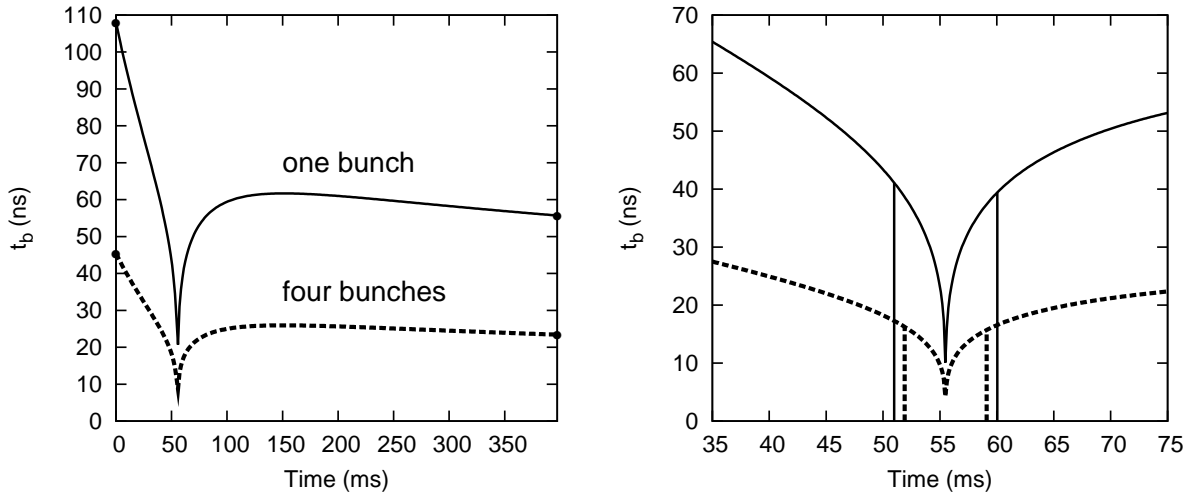


Figure 7: The full bunch length for the acceleration with one bunch,  $h = 5$  (solid lines), and with four bunches,  $h = 10$  (dashed lines). The total emittance is  $\epsilon_z = 0.85$  eV-s. The vertical lines in the right-hand side plot indicate the corresponding nonadiabaticity regions.

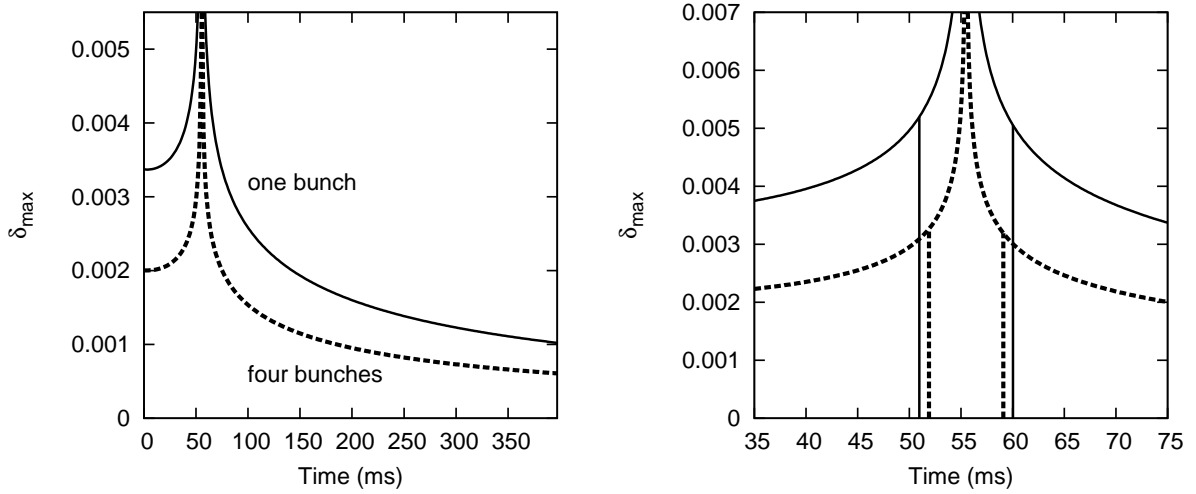


Figure 8: The half momentum spread for the acceleration with one bunch,  $h = 5$  (solid lines), and with four bunches,  $h = 10$  (dashed lines). The total emittance is  $\epsilon_z = 0.85$  eV-s. The vertical lines in the right-hand side plot indicate the corresponding nonadiabaticity regions.

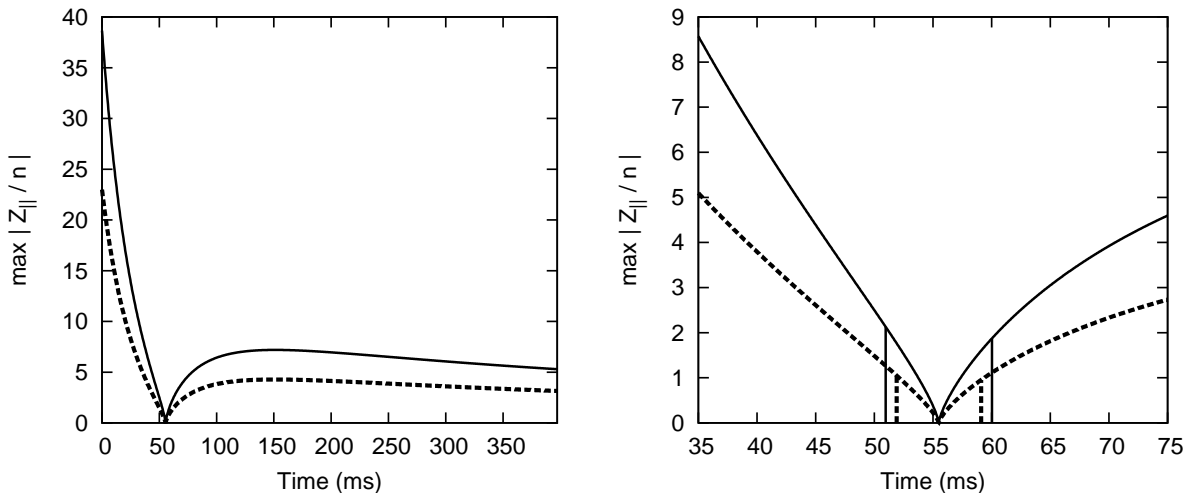


Figure 9: Stability boundary of the Boussard criterion for the longitudinal microwave instability for the acceleration with one bunch,  $h = 5$  (solid lines), and with four bunches,  $h = 10$  (dashed lines). The total emittance is  $\epsilon_z = 0.85$  eV-s. The vertical lines in the right-hand side plot indicate the corresponding nonadiabaticity regions.

## 5 Maximum Emittance for a Bunch Rotation at the Extraction for the Cycle with $\gamma_t = 8.9$

A non-matched bunch at the extraction energy with a bunch rotation before reaching the final bunch length  $t_b = 50$  ns allows for a larger longitudinal emittance during the transition and rf manipulations. The largest emittance is then given by the momentum acceptance  $\delta_{\max} = \pm 0.005$  and by the full bunch length  $t_b = 50$  ns at the extraction energy  $E_K = 29$  GeV,  $\epsilon_z = 3.74$  eV-s. However, this emittance produces  $\delta_{\max} = 0.011$  for the one-bunch acceleration and  $\delta_{\max} = 0.0065$  for the four-bunch acceleration near transition. This is above the momentum acceptance  $\delta_{\text{acc}} = 0.005$ . The upper limit of the longitudinal emittance for this scenario is thus given by the momentum spread near transition, and the resulting emittance is  $\epsilon_z = 2.22$  eV-s ( $A_z = 6.97$  eV-s, an increase by a factor 3.3),

one bunch	four bunches
$h = 5$	$h = 10$
$\epsilon_z = 2.22$ eV-s	$\epsilon_z = 0.56$ eV-s
$\eta_{\text{sc}} = 0.8$	$\eta_{\text{sc}} = 1.6$

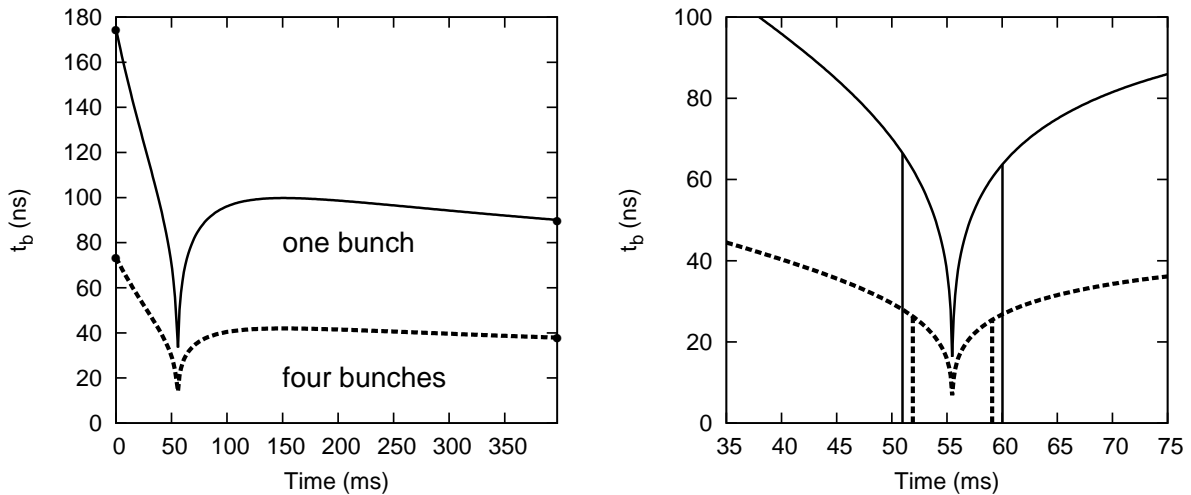


Figure 10: The full bunch length for the acceleration with one bunch,  $h = 5$  (solid lines), and with four bunches,  $h = 10$  (dashed lines). The total emittance is  $\epsilon_z = 2.22$  eV-s. The vertical lines in the right-hand side plot indicate the corresponding nonadiabaticity regions.

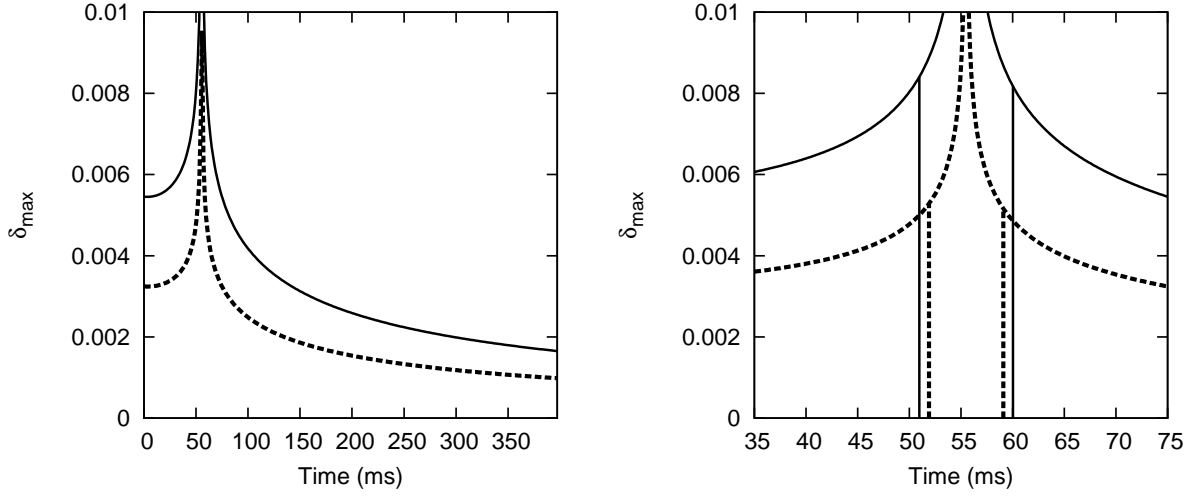


Figure 11: The half momentum spread for the acceleration with one bunch,  $h = 5$  (solid lines), and with four bunches,  $h = 10$  (dashed lines). The total emittance is  $\epsilon_z = 2.22$  eV-s. The vertical lines in the right-hand side plot indicate the corresponding nonadiabaticity regions.

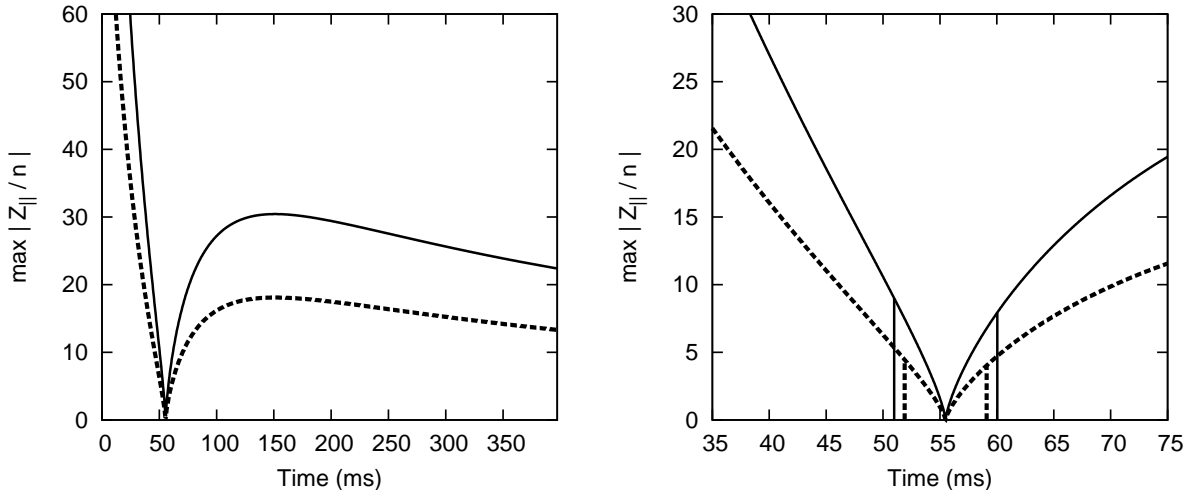


Figure 12: Stability boundary of the Boussard criterion for the longitudinal microwave instability for the acceleration with one bunch,  $h = 5$  (solid lines), and with four bunches,  $h = 10$  (dashed lines). The total emittance is  $\epsilon_z = 2.22$  eV-s. The vertical lines in the right-hand side plot indicate the corresponding nonadiabaticity regions.

## References

- [1] K.Y. Ng, *Physics of Intensity Dependent Beam Instabilities*, World Scientific, (2006)

[2] H. Damerou, et.al., CERN-ATS-Note-2012-064 MD (2012)

[3] Handbook of Accelerator Physics and Engineering, 2nd Ed, World Scientific, (2013)